Behaviour of steel with the metastable austenite during segmental grinding

LUCJAN DĄBROWSKI,
JERZY JELEŃKOWSKI,
MIECZYSŁAW MARCINIAK,
DOROTA SZCZĘŚNIAK

Lucjan Dąbrowski (ld@meil.pw.edu.pl), Jerzy Jeleńkowski (jjele@imp.edu.pl), Mieczysław Marciniak (mima@meil.pw.edu.pl), Dorota Szczęśniak, Warsaw University of Technology, Poland

How to cite: L. Dąbrowski, J. Jeleńkowski, M. Marciniak, D. Szczęśniak. Behaviour of steel with the metastable austenite during segmental grinding. Advanced Technologies in Mechanics, Vol 1, No 1 (1) 2014, p. 32–40.
DOI: http://dx.doi.org/10.17814/atim.y2014.iss1(1).art10

Abstract

The methods of the grinding process efficiency evaluation have been presented in this paper basing upon the temperature in the workpiece tool contact area. The technique of determining this temperature has also been given as a combination of analytical and experimental process. These are especially useful by properties and phase transformation investigations in the metastable austenite steels.

KEYWORDS: **Segmental grinding**, **Temperature registration**, **Metastable austenite**, **Deformation martensite**, **Phase transformation**

Introduction

Described in [1] conception of steel quenching by polishing finds special application during segmental grinding of the metastable austenite steel. These are high - strength steels developed mainly for military and spaceship application.

In the conventional heat treatment of the presented in table 1 steel, the austenite into thermal martensite transformation may occur when the amount of generated heat is sufficient to heat up austenite to the temperatures of 800 - 900 °C range. Following separation of phases reducing the alloy additions in the austenite results during cooling in its destabilization and transformation into martensite. Differently runs the process of the austenite into deformational martensite transformation, that means that during cold working and then heating the steel to the temperatures not exceed the Ms - Md range (Ms - the austenite into thermal martensite beginning temperature; Md - the lowest temperature of the cold worked austenite into martensite transformation). For most steels showed in table 1 the Md temperature is lower than 100 °C.

Table 1. The composition of the tested steels in wt. %

	C	S	P	Si	Mn	Ni	Ti	Mo	A1	Nb
N26MT2Nb	0,02	0,009	0,007	0,11	0,17	26,0	2,15	1,15	0,04	0,11
N26J2T3Nb	0,02	0,008	0,010	0,010	0,200	25,5	3,05	-	2,060	0,200

Martensitic transformations occurring during quenching and cold working have many common features. The nucleation of the deformation austenite takes place in the same areas where spontanic nucleation happens during cooling. The morphology of the deformed martensitic structures is close to thermal martensitic structures, because in both cases transformation temperature and deformation speed decides about it. Main difference in both martensitic structures exhibits in the phase boundaries area: these inducted with deformation are irregular, what reflects in advantageous changes of material properties. Fig. 1 shows that lower relative deformation speed ε' of the N26J2T3Nb steel increases microhardness $HV_{0,02}$ of the deformation martensite (lm, 2m, 3m) especially within 20 - 40 °C temperature range [2].

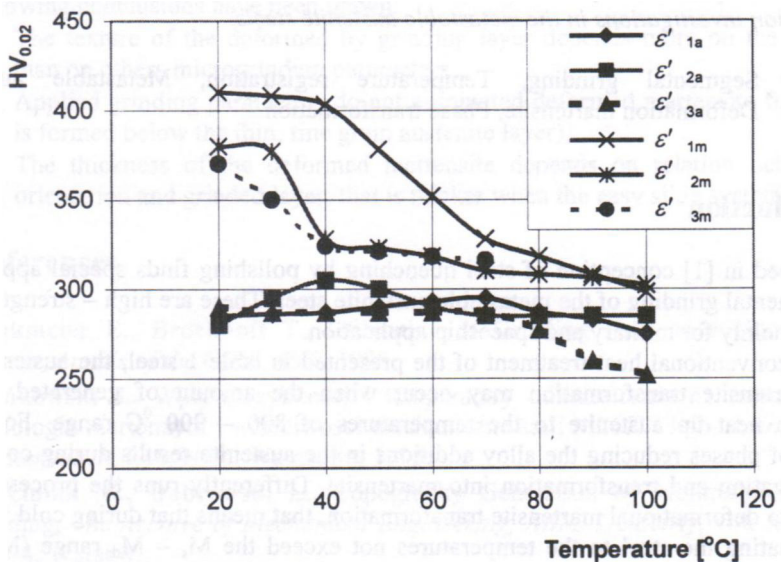

Fig. 1. *Martensite (m) and austenite (a) microhardness; conditioned by temperature and speed deformation: ε'_1= 8.3x10^{-4} [s^{-1}], ε'_2= 8.3xl0^{-3} [s^{-1}], ε'_3 = 8.3xl0^{-2} [s^{-1}]*

At the relative deformation speed ε'_1= 8.3x10^{-4} [s^{-1}], bigger microhardness of the deformation martensite was registered than at lower speed ε'_2= 8.3xl0^{-3} [s^{-1}], and ε'_3 = 8.3x10^{-2} [s^{-1}]. This is an important hint in regard to grinding process conditions, enabling to control both temperatures and material deformation speed of the machined layer of grinded object.

Computer simulation contact of the segmental grinding wheel with the machined surface

Fig. 2 shows a scheme of a segmental grinding wheel in nonconventional kinematic arrangement. By changing the position of the abrasive segments in the tool-in-use system has been estimated with the reference to the following processes [3]:

- changes of grain edge geometry,
- removal of built-up material from the grain face surface,
- control of the grain trajectory distribution on the machined surface.

In model testing, where the grain trajectory distribution on the machined surface is performed, computer visualization method has been applied. The program user can get immediate general assessment of trace concentration distribution on the machined surface for the given machining parameters. The rotation of the grinding segments around their axis has an effect on physical properties of the top layer of the machined workpiece. In model researches were found that essential effect of grain trajectories on the workpiece relative deformation [3]. That testified the height of material flashes at the edge of machining groove, which was characterized in Fig. 3a.

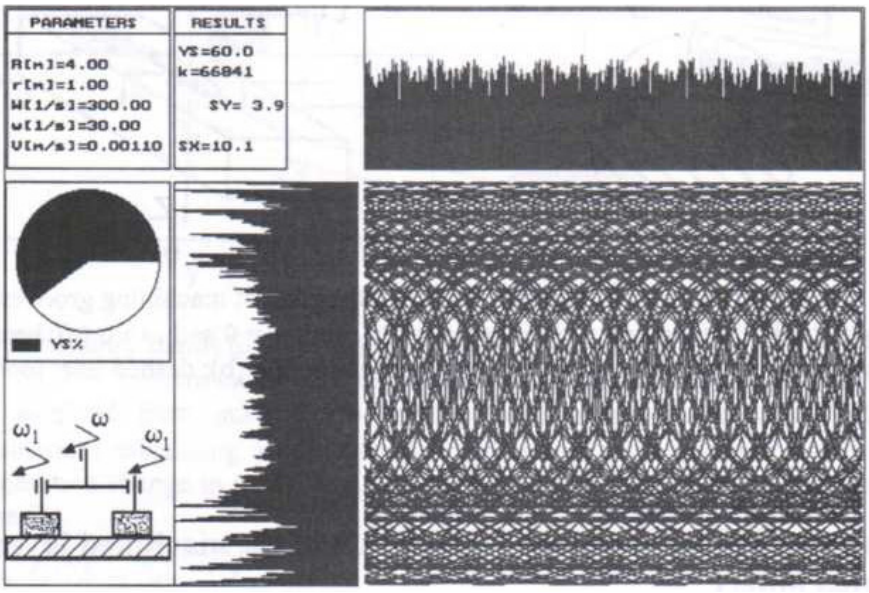

Fig. 2. *Computer drawing of grain trajectories*

In the following i = 5 contacts between tool point and material, the height H increases faster, when the tool point performs with linear velocity v [m/s] with no axial rotation (ω= 0). This means, that when the axial rotation of the tool $\omega > 0$, the relative deformation speed ε' changes due to the changing conditions of the micromachining process. Fig. 3a exposes that with increasing relative deformation speed ε'_1 of the metastable austenite steel intensifies its transformation into deformation martensite in low temperatures. These conditions are fulfilled hardness distribution tests around the machining groove resulting from a single contact between the tool point and the material (Fig. 3b) [4].

Registered increase of hardness in the area around the machining groove is a result only of a plastic deformation of this area, because generated heat doesn't increase momentary material temperature above 40 °C. To establish conditions of low temperature micromachining with non - conventional segmental grinding wheel a computerized measurement track enabling to control maximum grinding temperatures was applied.

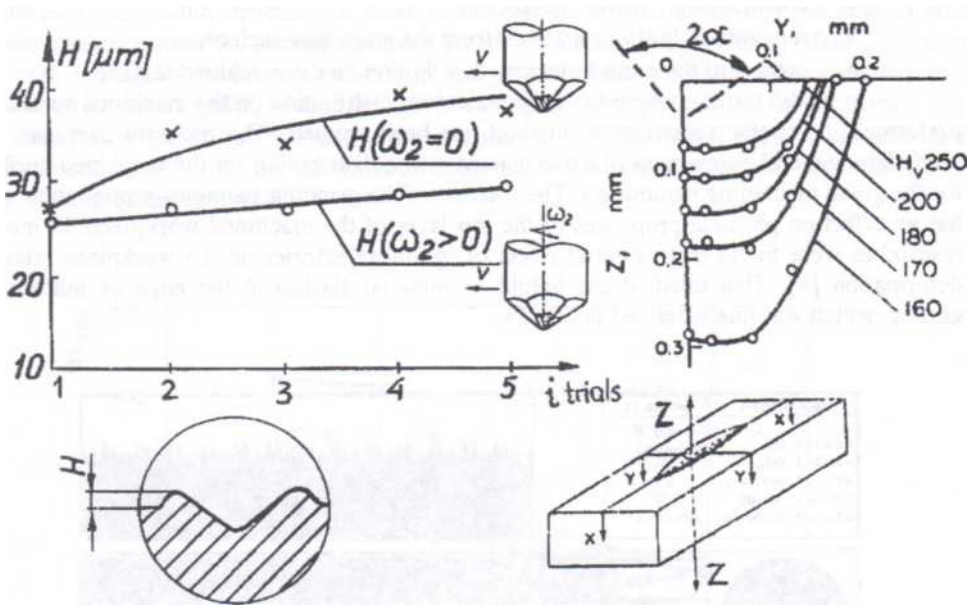

Fig. 3. *The height H of material flashes at the edge of machining grooves created by model-tool-point moving with linear velocity v and ω = 0 and ω > 0 (a); hardness distribution H_v around the machining groove in section YZ (b); dashed line: tool point profile for angle 2α*

Computerized temperature registration of the machined layer of the grinded object

In the area of contact between grinding wheel and machined object several heat sources are available corresponding to a number of active grindings grains. In the face segmental grinding, the total effect of these heats sources generating in the grinded object aransient temperature field is taken under consideration. In case, where the maximum temperature on the surface of a semi - infinite object does not equals 0, to calculate it, a nondimensional parameter *β* may be applied:

$$\beta = \frac{\theta - \theta_k}{\theta_o - \theta_k} = \text{erf} \quad u = \frac{2}{\sqrt{\pi}} \int e^{-u^2} du \tag{1}$$

where: θ, θ_o, $\theta_{k,}$ - measured surrounding and contact surface temperature,

$$u = \frac{1}{\sqrt{F_{oy}}} = \frac{1}{2\sqrt{a+t/y^2}},$$

F_{oy} - Fourier criteria, *a* - coefficient of temperature conduction, *t* - time of the temperature change in y function;

Parameter β changes in the following range: β =0 when $F_{0y} = \infty$, β =1 when F_{0y} =0. After transformation (1):

$$\theta_k = \frac{\theta - \beta\theta_0}{1-\beta} \tag{2}$$

Temperature θ_k is calculated based on temperatures measured in the low distances y_1 and y_2 from the grinded surface (Fig. 4).

In Fig. 5, temperatures θ_1, θ_2 changes run in the points of coordinate y_1, y_2 was observed.

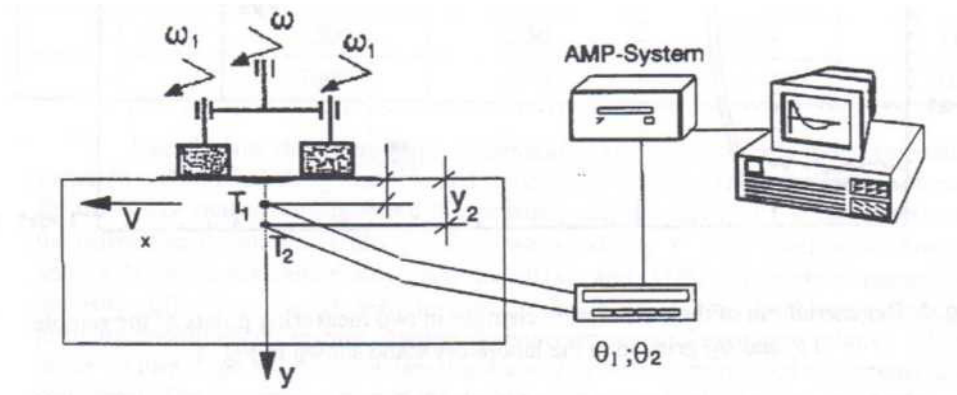

Fig. 4. *Laboratory stands for automatic temperature measurements in area of contact between the grinding wheel and the workpiece*

Data received from micro-thermocouples T_1, T_2 are automatically feeded into computer software calculating nondimensional parameter β. This software iterates time (t) of the temperature change in points y_1, y_2 in the way to minimize difference in the contact temperature (2).

$$\frac{\theta_1 - \beta_1\theta_0}{1-\beta_1} = \frac{\theta_2 - \beta_2\theta_0}{1-\beta_2}$$

In Fig. 5, temperatures θ_1, θ_2 changes run in the points coordinate y_1, y_2 was observed.

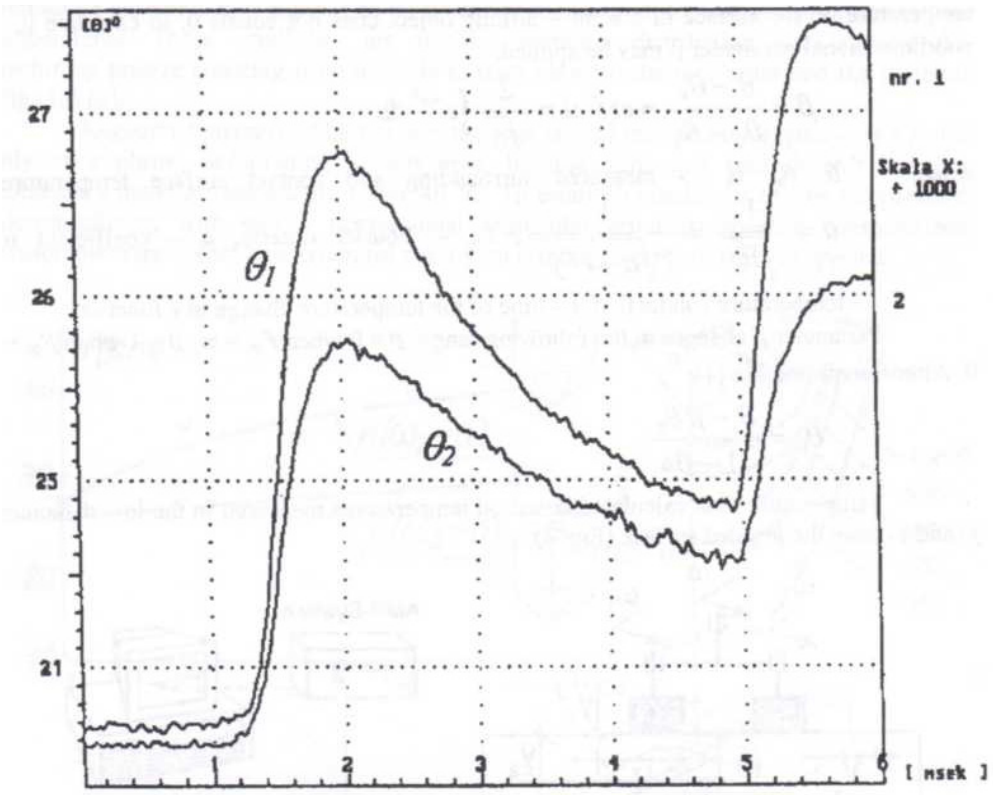

Fig. 5. *Registered run of the temperature changes in two measuring points of the sample (θ_1 and θ_2) grinded in the laboratory stand shown in Fig. 4*

Maximum temperatures are registered for following segments of grinding wheel, passing above thermo-couples located under the grinded surface. Contact temperature θ_k of the grinding wheel and workpiece calculated automatically indicates for conditions of deformation of the grinded material layer. During nonconventional grinding, when grinding segments rotate axially $\omega_t > 0$, Fig. 3, the temperature θ_k is even 40 % lower than when grinding with axially fixed ($\omega_t = 0$) segments. In these conditions, responsible for the state of outer layer is rather plastic deformation of grinded material, than grinding temperature.

Microstructure and features of the top layer of the N26MT2 steel grinded with the nonconventional grinding wheel

Assessment of the segmental grinding parameters influence on the microstructure and hardness distribution in top layer of the N26MT2Nb steel was realized according to data from table 2 by constant grinding depth a_e = 0,02 mm. The average temperatures of the grinded layer θ_k were calculated for the registered higher temperatures $\theta_{1, \theta 2}$ by the second passage of grinded wheel (Fig. 5).

Table 2. Example parameters of segmental grinding of the N26MT2Nb steel (Fig. 2) and calculated temperatures of outer layer

Samples No	Parameters			
	ω rpm.	ωt rpm.	vf m/min.	θk °C
1	3500	500	1.5	210
2	3000	500	3.0	80
3	2500	250	3.0	110
4	2000	250	1.5	100

Samples for the microscope observation and microhardness measurements were prepared with the polishing machine and etched with NITAL. The same samples were used for the X ray analysis to registered the structure changes caused by grinding process. For the diffraction registration CuK_α radiation was used. Fig. 6 show interference from $(111)_\gamma$ and $(002)_\gamma$ of the austenite family plane and $(011)_\alpha$ and $(110)_\alpha$ deformation martensite. The intensity differences, better seen in $(002)_\gamma$ pike revealed considerable influence of the grinding conditions on texture changes in deformed layer. The biggest relative differences in the texture stage are between samples 4 and 2, which were worked in extreme different conditions. The martensite share in the deformed layer probably changes not much.

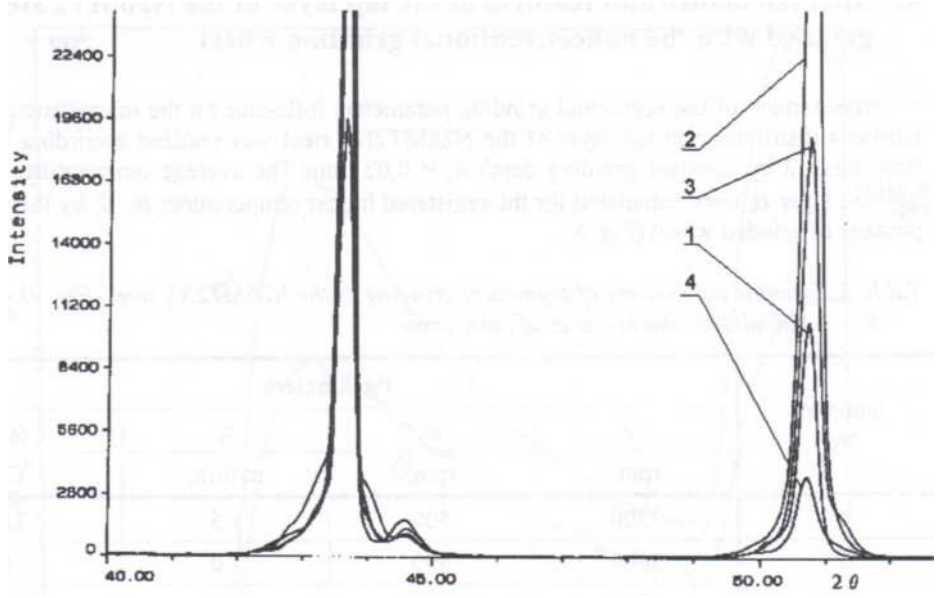

Fig. 6. *Difractogram of the N26MT2Nb layer (samples 1, 2, 3, 4, table 2). Below figures show interference from $(111)_\gamma$ and $(002)_\gamma$ of the austenite family plane and $(011)_\alpha$ and $(110)_\alpha$ deformation martensite*

The intensity of the martensite pikes (as seen in microstructure photographs) is low because martensite is screened by thin and fine grain layer of the austenite. Martensite lies in slide strips below austenite layer. The range of slide strips depends on grain orientation relative to grinded layer, in which martensite is generated (Fig. 7 a, b, c).

The martensite occurs under that layer in slide strips. The slide strips range depends on grain orientation relatively to grinded layer, in which the martensite is generated (Fig. 7a, b). When that orientation promotes easy slide systems the martensite layer thickness is bigger. The temperature in which the fine - grain austenite layer is formed is higher than M_d temperature. Relatively high temperature, high deformation speed and fine grain give the opportunity to nucleation of the deformed martensite. The profitable conditions for deformed martensite transformation take the place in distance of 4 - 8 μm from the grinded layer (Fig. 7c).

Microhardness measurements are shown in Fig. 8. Comparing data in graph and microstructure pictures a good comformable to phase constitution, samples deformation effect and to microhardness were found. Samples with thicker layer of the deformed martensite are harder.

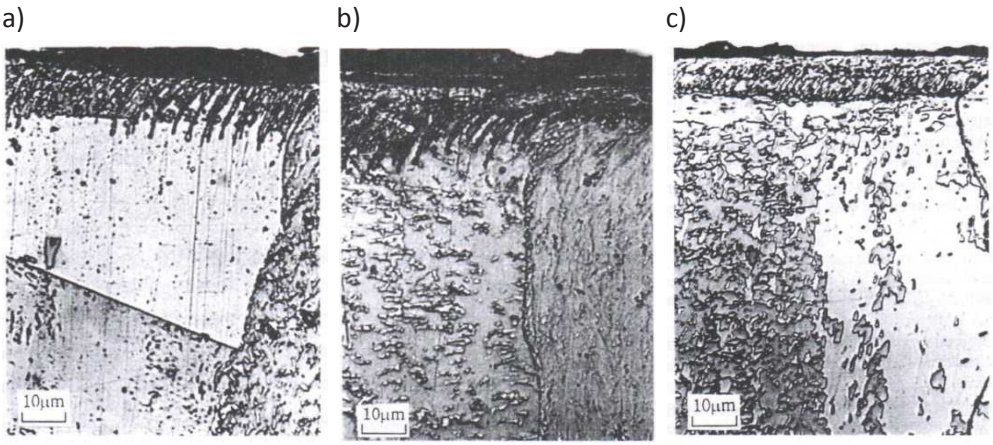

Fig. 7. *Microslructure of the coarse grain structure layers of the deformed by segmental grinding metastable austenite. Outer: very thin layer of the fine grain austenite. Under: deformed martensite seen in slide strips (a, b, c - samples No. 2, 3 and 4 in table 2)*

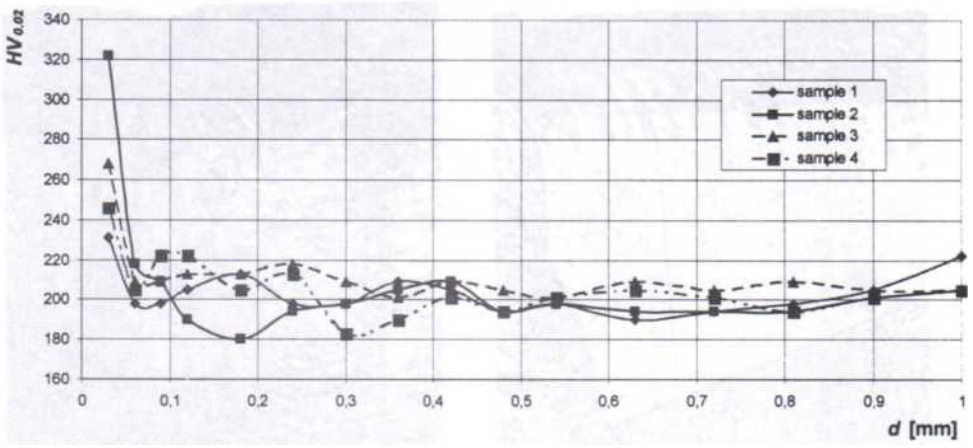

Fig. 8. *The microhardness distribution in outer layer of the N26MT2Nb grinded steel*

Conclusions

The following conclusions have been drawn:

- The texture of the deformed by grinding layer depends more on the feed speed than on others microgrinding parameters,
- Applied grinding parameters do not eliminated deformed martensite forming (that is formed below the thin, fine grain austenite layer),
- The thickness of the deformed martensite depends on relation between grain orientation and grinded layer; that is thicker when the easy slide system is started.

References

Brinkmeier E., Brockhoff T., Utilization of Grinding Heat as a New Treatment Process, *Annals of the CIRP*, 45/1, 1996.

Jeleńkowski J., Wpływ szybkości i temperatury odkształcania na temperaturę M_d, morfologie martenzytu i właściwości mechaniczne stali M26J2T3Nb, *Archiwum Nauki o Materiałach*, t. 16, No. 4, Warszawa, 1995.

Marciniak M., Dąbrowski L., Topography Generation by Nontraditional Surface Grinding, *The Archive of Mechanical Engineering, ABM*, Quarterly, vol. XLII (1995), No 3-4, Warsaw.

Yoshiro K., Mamoru I., Deformation work in abrasive cutting. *Inst. J. Mach. Tool Des. and Res.* vol.16, No 3, 1976.